



ISOLATION, CHARACTERIZATION, AND MOLECULAR DOCKING STUDIES OF CHLOROFORM FRACTIONATE OF *PSAMMOGETON BITERNATUM EDGEW*

Nida Munir¹, Bashir Ahmad^{1*}, Aishma Khattak², Nida Gul³, Muhammad Idrees⁴,
Sudhair Abbas Bangash⁵

¹Centre of Biotechnology and Microbiology, University of Peshawar

^{2*}Department of Bioinformatics, Shaheed Benazir Bhutto Women University Peshawar

³Department of Environmental Sciences University of Swabi.

⁴Department of Health and biological sciences, Abasyn university Peshawar.

⁵Faculty of Life Science, department of pharmacy sarhad University of science and information technology, Peshawar.

*Corresponding Author: Bashir Ahmad

Email: bashidr2015@yahoo.com

Abstract

Medicinal plants have been widely used in the treatment of various diseases for human health. The present aim of this study was to investigate and identify the bioactive compounds from crude extracts of *Psammogeton biternatum Edgew*. It belongs to the family Apiaceae. There are numerous advanced techniques were used like NMR and HMBC. Three new pure compounds i.e., compound 1, compound 2 and compound 3 were isolated from the chloroform fraction of the plant. These compounds were screened for enzyme inhibition which was found more potent than the standard. In addition, an *in silico* molecular docking analysis was also performed with the target enzyme α -glucosidase which potential target for diabetic patients. Among all the three compounds, compound 3 showed the best docking score of -7.6 kcal/mol with the target enzyme. Moreover, in the future, this study can shed light on the development of plant therapeutics for diabetic patients.

Keywords: Medicinal plants, *Psammogeton biternatum Edgew*, NMR, HMBC, molecular docking, and α -glucosidase

1. Introduction

Psammogeton biternatum Edgew belongs to family Apiaceae/ Umbelliferae which is the major group of angiosperms (flowering plants), commonly in central areas of Asia including Iran, Afghanistan, Turkmenistan, and Pakistan (Rahimi-Nasrabadi et al., 2009). The selected plant *P. biternatum Edgew*. commonly known as “Sparki” and “Liwany Gajara” locally. It is an annual herb and about 15 to 20cm in length. The flowers are small and white or pink colour. Flowering period is March–April. Medicinally it is very important plant as it is used in treatment of malaria, cough, typhoid, and chest problems (Assiry et al., 2023; Aziz-UL-Ikram et al., 2015; Hasan et al., 2023; Javed et al., 2022; Tariq et al., 2020). *P. biternatum Edgew*. seeds are also ground and mixed in water and sugar and taken orally after delivery for postpartum infections (Bibi et al., 2017). One of studies in streptozotocin induced albino rats showed that whole plant extract of *P. biternatum Edgew* showed strong anti-diabetic results compared to the standard drug metamorphine (Ajajib et

al., 2019). Three pure compounds were isolated from whole plant and were identified by spectroscopic analysis and chemical methods. The docking results showed great interactions of compound 3 with the target enzyme α -glucosidase enzyme. It was concluded that in future this study could provide platform for the detailed screening of these phytochemicals for the therapeutic purposes and for the treatment of diabetic patients.

2. Experimental

2.1 Plant material

Psammogeton biternatum Edgew was collected from different regions of District Bannu for present study. Plant was identified from Department of Botany of University of Peshawar. The whole plant (4kg) of *P. biternatum* was cleaned and shade dried. It was later macerated in ethanol solvent. The extract was dried on rotary evaporator to get final extract which weighed approximately 800 grams.

2.2 Extraction and fractionation

The crude methanolic extract was then filtered and was soaked in 500 milliliters distilled water. The suspensions were then processed to make different fractions containing *n*-hexane (3 × 400 ml), chloroform (3 × 400 ml), ethyl acetate (3 × 400 ml), thus we obtained 150 g from *n* hexane, 120 g from chloroform, 109 g from ethyl acetate and 421 g from aqueous fractions. The chloroform fraction of was used for further study (Afzal et al., 2023; Assiry et al., 2023; Ramzan et al., 2022).

2.3 Isolation and purification of Compounds

The chloroform fraction was accessed to column chromatography which led to the isolation and refinement of several components of plant extract. In the whole chromatography process, two solvent systems were used. First system used was of *n*-hexane and ethyl acetate and the second solvent system used was of chloroform and methanol. The elutions gathered from each solvent system were further purified by the help of thin layer chromatography which confirmed the presence of three compounds i.e., Compound 1 (1.23g), Compound 2 (1.22 g) and Compound 3 (1.2 g). Identification and spectral analysis of these three compounds was performed by the help of various advanced techniques including NMR, HMBC, UV spectroscopy and FT-IR (Ahmed et al., 2022; Amin et al., 2023; Anis et al., 2021).

2.3.1 Compound 1

White crystalline mass; molecular ion peak at m/z 414.12 a.m.u, molecular formula C₂₉H₅₀O, FT-IR absorption peaks at 3550, 2935 and 2990 and UV spectroscopy absorption peaks at 248 and 266. Structure of compound 1 was identified by HBMC spectra which showed similarity with literature value (Table 1).

2.3.2 Compound 2

White needle like crystals; molecular ion peak at m/z 412.01 a.m.u, molecular formula C₂₉H₄₈O, FT-IR absorption peaks at 3550, 3490 and 1679, UV spectroscopy absorption peak at 243 and 267. Structure of compound 2 was identified by HBMC spectra which showed similarity with literature value (Table 2).

2.3.3 Compound 3

White amorphous mass; molecular ion peak at m/z 456.00 a.m.u, molecular formula C₃₀H₄₈O₃, FT-IR absorption peaks at 3550, 3505, 2992 and 1676, UV spectroscopy absorption peak at 248 and 262. Structure of compound 3 was identified by HBMC spectra which showed similarity with literature value (Table 3).

2.4 Molecular Docking Simulations

Docking simulations were carried out through AutoDock Vina software (Trott et al., 2010) to elucidate the binding mode of α -glycosidase with novel compounds (1-3). The crystal structure of the protein was retrieved from the Protein Data Bank (PDB code = 5NN8) with a resolution of 2.45 Å, whereas the 3-D structure was visualized, and the solvent molecules were removed from the protein molecule. The protein structure geometry optimization and refinement were performed through Swiss PDB viewer v4.1.0 program (Kaplan and Littlejohn, 2001). The compound 1 and standard (acarbose) structures were prepared by using Chem sketch (Li et al., 2004) and Avogadro's software (Hanwell et al., 2012). PyRex tool was connected with AutoDock Vina (Wargasetia et al., 2018). The addition of hydrogen and calculation of gasteiger charges were performed. All rotatable bonds of molecules were defined by default of the software, it was allowed to rotate during the automated docking process. Then both the prepared protein and the small molecule structures were used for calculating energy grid maps. A grid box size of 70 × 70 × 70 Å points with a grid spacing of 0.4 Å was considered focusing on the center. It was defined as the center of the co-crystallized inhibitor (Acarbose). Numerous clusters and binding affinities were found for docked compound (Laskowski and Swindells, 2011) in which the best conformers were choose due to the lower docked free energy and top-ranked cluster to perform docking analysis with LIGPLOT+ version v.1.4.5 and PyMOL version 1.7.2. Authenticity of docking method was tested by means of a known co-crystallized ligand (Acarbose) of the enzyme. The structure of Acarbose was extracted from the binding pocket and re-docked to the α -glycosidase enzyme.

3. Results and Discussion

Compound **1** was obtained as white crystalline mass. The mass spectroscopy showed molecular ion peak at m/z 414.12 a.m.u, which consistent with molecular formula C₂₉H₅₀O. The FT-IR spectroscopy revealed absorption peaks at 3550 which indicated the presence of OH, 2935 and 2910 for CH saturated stretching, 1680 for unsaturated double bond. The UV spectroscopy of compound 1 showed absorption peak at 248, 266 for unsaturated double bond. The proton and carbon NMR spectroscopy data was like the reported data. We have identified the structure of compounds 1 by HBMN spectra which showed similarity with literature value (Amin et al., 2023; Ramzan et al., 2022). Thus, the chemical structure of 17-(5-ethyl-6-methylheptan-2-yl)-10,13-dimethyl-2,3,4,7,8,9,10,11,12,13,14,15,16,17-tetradecahydro-1H-cyclopenta[a]phenanthrene-3-ol was characterized by comparing physical and spectral data with reported data (Table 1) (Fig 1, 2).

Compound **2** was obtained as white needle like crystals. The mass spectroscopy showed molecular ion peak at m/z 412.01 a.m. u, which consistent with molecular formula C₂₉H₄₈O. The FT-IR spectroscopy revealed absorption peaks at 3550 which indicated the presence of OH, 3490 and 2990 for CH saturated stretching, 1679 for unsaturated double bond. The UV spectroscopy of compound 2 showed absorption peak at 243, 267 for unsaturated double bond. The proton and carbon NMR spectroscopy data was like the reported data. We have identified the structure of compounds 2 by HBMN spectra which showed similarity with literature value. Thus, the chemical structure of (E)- 17-(5-ethyl-6-methylhept-3-en-2-yl)-10,11,12,13,14,15,16,17-tetradecahydro-1H-cyclopenta[a]phenanthrene-3-ol was characterized by comparing physical and spectral data with reported data (Table 2) (Fig 1, 2).

Compound **3** was obtained as white amorphous mass. The mass spectroscopy showed molecular ion peak at m/z 456.00 a.m. u, which consistent with molecular formula C₃₀H₄₈O₃. The FT-IR spectroscopy exhibited absorption peaks at 3550 which indicated the presence of OH, 3505 and 2992 for CH saturated stretching, 1676 for unsaturated double bond. The UV spectroscopy of compound 3 showed absorption peak at 248, 262 for unsaturated double bond. The proton and carbon NMR spectroscopy data was like the reported data. We have identified the structure of compounds 3 by HBMN spectra which showed similarity with literature value. Thus the chemical structure of 3a-(hydrperoxymethyl)-5a,5b,8,8,11a-pentamethyl-1-(prop-1-en-2-

yl)icosahydro-1Hcyclopenta[a] chrysene-9-ol was characterized by comparing physical and spectral data with reported data (Table 3)(Fig 1, 2).

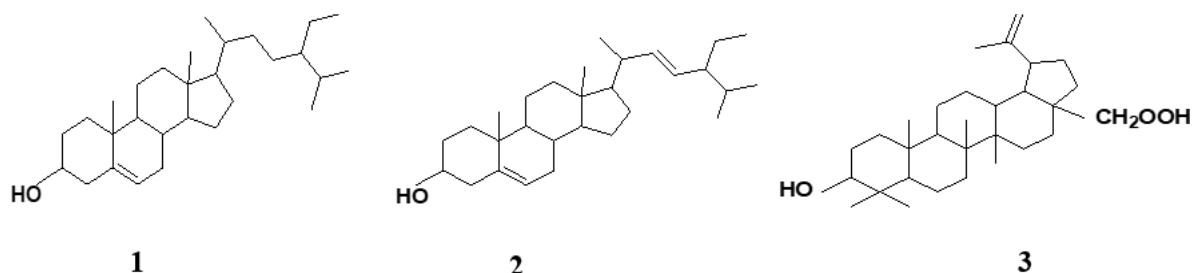


Figure 1. Chemical structure of compound (1-3) isolated from *Psammogeton biternatum* Edgew.

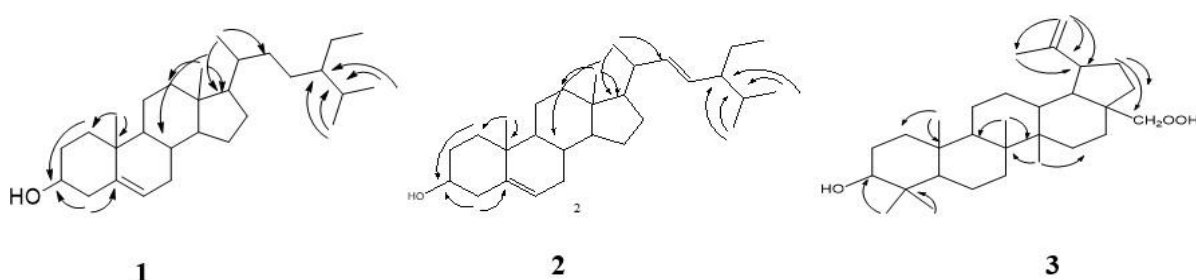


Figure 2. Key HMBC correlations of compound (1-3).

Table 1. NMR spectroscopy data of compound 1

No	δ H	δ C	Types	HMC correlations
1	1.07 dd (J=3.6, 6.12)	37.4	CH ₂	C-3, C5, C19
2	1.24, 1.49, m	31.9	CH ₂	-
3	3.53, m	71.8	CH ₂	-
4	2.01, t, (8.89); 1.99, (d; j=3.14)	42.5	CH ₂	C-2, C-3, C-5, C-6, C-10
5	-	140.9	C	-
6	2.36, d, (j=3.5)	121.3	CH	C-4, C-8, C-10
7	1.45, m	32.3	CH ₂	-
8	1.43, m	32.00	CH	-
9	0.85, m	50.6	CH	-
10	-	37.2	C	-
11	1.50, m, 1.48, m	21.0	CH ₂	-
12	2.19, d, (j=2.1); 2.26, dd, (J=2.2, 3.2)	42.4	CH ₂	-
13	-	39.9	C	-
14	0.96, m	56.9	CH	-
15	1.57, m	24.4	CH ₂	-
16	1.24M	28.4	CH ₂	-
17	1.08, dd, (J=7.9, 3.49)	56.2	CH	-
18	0.67, s	12.1	CH ₃	C-12, C1-14, C-17
19	0.98, S	19.5	CH ₃	C-1, C-9
20	1.35, S	36.3	CH	-
21	0.92, d, (J=5.26)	18.9	CH ₃	C-17, C-20
22	1.28, m	34.1	CH ₂	-
23	1.15, m	26.13	CH ₂	-
24	0.93, m	45.91	CH	-
25	1.26, m	29.21	CH	-

26	0.80, d, (J=6.9)	19.12	CH ₃	C-24, C-25
27	0.82, d, (J=5.59)	23.13	CH ₃	C-24, C-25
28	1.23, m	23.13	CH ₂	-
29	0.83, T, (J=7.6)	12.07	CH ₃	C-24, C-25, C-28

Table 2. NMR spectroscopy data of compound 2

No	δ H	δ C	Types	HMC correlations
1	1.07 dd (J=3.6, 6.12)	37.4	CH ₂	C-3, C5, C19
2	1.24, 1.49, m	31.9	CH ₂	-
3	3.53, m	71.8	CH ₂	-
4	2.01, t, (8.89); 1.99, (d; j=3.14)	42.5	CH ₂	C-2, C-3, C-5, C-6, C-10
5	-	140.9	C	-
6	2.36, d, (j=3.5)	121.3	CH	C-4, C-8, C-10
7	1.45, m	32.3	CH ₂	-
8	1.43, m	32.00	CH	-
9	0.85, m	50.6	CH	-
10	-	37.2	C	-
11	1.50, m, 1.48, m	21.0	CH ₂	-
12	2.19, d, (j=2.1); 2.26, dd, (J=2.2, 3.2)	42.4	CH ₂	-
13	-	39.9	C	-
14	0.96, m	56.9	CH	-
15	1.57, m	24.4	CH ₂	-
16	1.24M	28.4	CH ₂	-
17	1.08, dd, (J=7.9, 3.49)	56.2	CH	-
18	0.67, s	12.1	CH ₃	C-12, C1-14, C-17
19	0.98, S	19.5	CH ₃	C-1, C-9
20	1.35, S	36.3	CH	-
21	1.2 d, (J=7.00)	21.5	CH ₃	C-17, C-20
22	5.05, dd, (J=15, 9)	139.5	CH	-
23	1.18, dd, (J=15, 9)	129.7	CH	-
24	0.93, m	52.9	CH	-
25	1.26, m	30.4	CH	-
26	0.80, d, (J=6.9)	19.12	CH ₃	C-24, C-25
27	0.82, d, (J=5.59)	23.13	CH ₃	C-24, C-25
28	1.23, m	23.13	CH ₂	-
29	0.83, T, (J=7.6)	12.07	CH ₃	C-24, C-25, C-28

Table 3. NMR spectroscopy data of compound 3

No	δ H	δ C	Types	HMC
1		38.7	CH ₂	
2		27.6	CH ₂	
3	4.65, brs	78.7	CH	
4		38.9	C	
5		55.4	CH	
6		18.3	CH ₂	
7		34.3	CH ₂	
8		40.7	C	

9		50.6	CH	
10		37.3	C	
11		20.9	CH ₂	
12		25.4	CH ₂	
13		38.4	CH	
14		42.4	C	
15		30.6	CH ₂	
16		33.0	CH ₂	
17		56.4	C	
18		47.8	CH	
19	3.08, t, (J=10.8 Hz)	49.2	CH	C-21, C-22, C-28
20	-	150.7	C	-
21	1.36, s	37.2	CH ₂	C-22, C-28
22	1.52, s	29.7	CH ₂	C-28
23	0.88, s	27.9	CH ₃	C-3, C-4
24	0.89, s	15.6	CH ₃	C-3, C-5
25	0.86, s	15.9	CH ₃	C-1, C-10
26	0.97, s	16.2	CH ₃	C-8, C-9
27	0.95, s	15.0	CH ₃	C-8, C-14
28	-	180.1	C	C-13, C-14, C-15
29	4.65, s	110.1	CH ₂	C-19, C-20, C-30
30	1.63, s	19.4	CH ₃	C-20

The isolated compounds were screening for α -Glucosidase inhibitory potential. The tested compounds (1-3) showed excellent effect. Among the tested compounds, compound 1 exhibited maximum effect with IC₅₀ value 145.87±2.98 followed by compound 2 having IC₅₀ value 116.98±2.09. The compound 3 showed good activity with IC₅₀ value 105.09±1.98. The acarbose was found more active as compared to tested compounds (Table 4)

Table 4. α -Glucosidase activity of isolated compounds (1-3) from *Psammogeton biternatum* Edgew.

Samples	Concentration	% inhibition	IC ₅₀ μ M
Compound 1	0.2 μ M	71.65	105.09±1.98
Compound 2	0.2 μ M	76.43	116.98±2.09
Compound 3	0.2 μ M	83.87	145.87±2.98
Standard drug	0.2 μ M	91.23	841.98±2.09

α -Glucosidase (EC 3.2.1.20) catalyzes the hydrolytic reaction to release α -glucose from the non-reducing part of the substrate. The enzyme can perform transferring and condensation reactions, as well as the hydration of D-glucal. α -Glucosidases are classified into two groups, GH-family 13 and 31, based on the sequence homology. These enzymes which are obtained from plant, animal, mold, bacteria, and human α -glucosidases as well as α -glucan lyase (EC 4.2.2.13) and α -xylosidase are members of GH-family 31 (Uddin et al., 2012). These are membrane-bound enzymes located at the epithelium of the small intestine and considered as the key enzymes of carbohydrate digestion. Recently, the human α -glucosidase binding interactions with competitive inhibitor acarbose was investigated (Frandsen et al., 2000). Besides the conserved catalytic GH-31 domain (residues 334-779), a variable loop originating from the N-terminal domain (residues 271-288) contribute towards the architecture of substrate binding site. Secondary structure elements consist of 10 alpha helices and 28 small beta sheets with intermittent loop regions. Human α -glucosidase active site is a pocket formed mainly by the GH31 domain residues, specifically Asp398, Asp587, His645, and Arg571.

Residues Trp472 and Phe518 come into proximity to the opening of the active site and can contribute towards the architecture of the substrate binding site. Additional residues lining the sugar binding site include Asp511, Trp370, Ile435, Trp509, and Met512. Study of virtual screening between human α -glucosidase and acarbose revealed that the residues Asp547, Asp511, Asp398, Arg571, and His645 are important for binding interaction (Tundis et al., 2010). The docking results revealed that the compounds 1 used in this study showed a promising interaction of α -glucosidase enzyme. Molecular insights based on docking study revealed the reason behind better binding affinity of compound 1 to show hydrophobic interactions with the following moieties (Trp376, Trp481, Phe525, Ser676, Leu677 and Leu678). Compound 2 showed important interactions with the critical amino acid residues. Apart from this favorable contact reasonable hydrophobic interactions were also observed from the surrounding residues, such as Trp376, Arg411, Trp481, Phe525, Leu677 and Leu678. In case of compound 3, methoxy group played a vital role in binding with α -glucosidase enzyme. Similarly, these functional moieties were surrounded through hydrophobic contacts (Trp376, Arg411, Lys479, Phe525, and Leu678). Also, a hydrogen bonding with distance of 2.85Å with Trp481 and Compound 1 main methoxy group was also displayed. This study highlighted the potential of steroidal alkaloids as possible treatment of diabetes mellitus agents by targeting α -glucosidase enzyme (Fig 3) (Table 5).

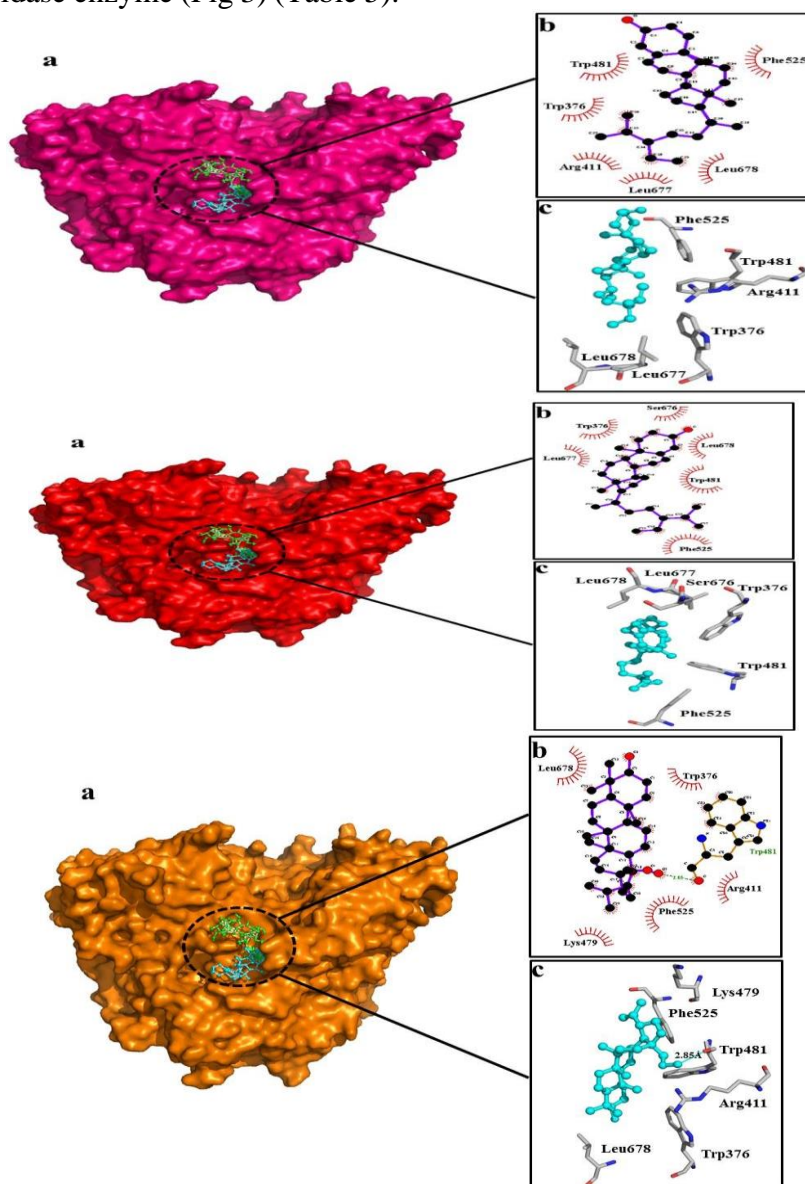


Figure 3. Molecular Docking poses of Compound (1-3) with the target receptor.

Table 5. Docking statistics of Compounds (1-3) and standard (Acarbose) against the α -glycosidase enzyme.

Compounds	Hydrogen bonding and hydrophobic contact residues	B. Affinity (Kcal/mol)
1	Trp376, Trp481, Phe525, Ser676, Leu677 and Leu678	-7.2
2	Trp376, Arg411, Trp481, Phe525, Leu677 and Leu678	-7.1
3	Trp481(2.85Å), Trp376, Arg411, Lys479, Phe525, and Leu678	-7.6
Acarbose (Standard)	Asp547, Asp511, Asp398, Arg571, and His645	-7.4

4. Conclusion

Around the globe, people are safely using and trusting herbal medicine for the treatment of various health problems. Also, herbal medications are the most used alternative therapy for lowering blood sugar in diabetic patients. Hence, preliminary results obtained from this study of isolated compounds can be used for designing novel inhibitors for an α -glucosidase enzyme which is a potential target for diabetic patients.

References:

- Afzal, M., A.S. Khan, B. Zeshan, M. Riaz, U. Ejaz, A. Saleem, R. Zaineb, H.A. Sindhu, C.Y. Yean, and N. Ahmed. 2023. Characterization of bioactive compounds and novel proteins derived from promising source *Citrullus colocynthis* along with in-vitro and in-vivo activities. *Molecules*. 28:1743.
- Ahmed, N., M.I. Karobari, A. Yousaf, R.N. Mohamed, S. Arshad, S.N. Basheer, S.W. Peeran, T.Y. Noorani, A.A. Assiry, and A.S. Alharbi. 2022. The antimicrobial efficacy against selective oral microbes, antioxidant activity and preliminary phytochemical screening of *Zingiber officinale*. *Infection and Drug Resistance*:2773-2785.
- Ajaib, M., M. Changaiz, M.A.I. Aziz-ul-Hassan, and K.H. Bhatti. 2019. EVALUATION OF THE ANTIOXIDANT AND ANTIDIABETIC PROPERTIES OF PSAMMOGETON BITERNATUM EDGEW. IN STREPTOZOTOCIN INDUCED DIABETIC MALE RATS. *INT. J. BIOL. BIOTECH.* 16:95-100.
- Amin, Z.S., M. Afzal, J. Ahmad, N. Ahmed, B. Zeshan, N.H.H.N. Hashim, and C.Y. Yean. 2023. Synthesis, Characterization and Biological Activities of Zinc Oxide Nanoparticles Derived from Secondary Metabolites of *Lentinula edodes*. *Molecules*. 28:3532.
- Anis, S., M.M. Khan, Z. Ali, A. Khan, H.M. Arsalan, S. Naeem, I. Saleem, S. Qamar, M.M. Khan, and A. Ahmad. 2021. Novel corona virus disease (COVID-19): An updated review on epidemiology, pathogenicity, clinical course, treatments, migrant health concerns and risk factors predictions. *Pak. J. Pharm. Sci.* 34:1807-1822.
- Assiry, A.A., N. Ahmed, A. Almuaddi, A. Saif, M.A. Alshahrani, R.N. Mohamed, and M.I. Karobari. 2023. The antioxidant activity, preliminary phytochemical screening of *Zingiber zerumbet* and antimicrobial efficacy against selective endodontic bacteria. *Food Science & Nutrition*.
- Aziz-UL-Ikram, N.B.Z., Z.K. Shinwari, and M. Qaiser. 2015. Ethnomedicinal review of folklore medicinal plants belonging to family Apiaceae of Pakistan. *Pak J Bot.* 47:1007-1014.
- Bibi, T., M. Ahmad, I. Ahmadbaloch, S. Muhammad, and R. Manzoor. 2017. Ethnomedicinal uses of plants for child birth and postpartum recovery in District Pishin, Northern Balochistan, Pakistan. *Int J Biol Pharm Allied Sci.* 6:1730-1760.
- Frandsen, T.P., F. Lok, E. Mirgorodskaya, P. Roepstorff, and B. Svensson. 2000. Purification, enzymatic characterization, and nucleotide sequence of a high-isoelectric-point α -glucosidase from barley malt. *Plant physiology.* 123:275-286.
- Hanwell, M.D., D.E. Curtis, D.C. Lonie, T. Vandermeersch, E. Zurek, and G.R. Hutchison. 2012. Avogadro: an advanced semantic chemical editor, visualization, and analysis platform.

Journal of cheminformatics. 4:1-17.

11. Hasan, Z., B. Zeshan, A. Hassan, N.H.A. Daud, A. Sadaf, and N. Ahmed. 2023. Preparation and characterization of edible whey protein nanofibrils and efficacy studies on the quality and shelf-life of chilled food products. *Journal of Food Safety.* 43:e13034.
12. Javed, F., Z. Ali, S. Ali, N. Ahmed, M.K. Alam, Y. Mahmood, and A. Wali. 2022. BARLEY BRAN, A NOVEL AGRICULTURAL WASTE FOR THE IMPROVED PRODUCTION OF AN EXTRACELLULAR LACCASE FROM A SOIL-INHABITED *Penicillium* spp. *Journal of microbiology, biotechnology and food sciences.* 12:e3631-e3631.
13. Kaplan, W., and T.G. Littlejohn. 2001. Swiss-PDB viewer (deep view). *Briefings in bioinformatics.* 2:195-197.
14. Laskowski, R.A., and M.B. Swindells. 2011. LigPlot+: multiple ligand–protein interaction diagrams for drug discovery. ACS Publications.
15. Li, Z., H. Wan, Y. Shi, and P. Ouyang. 2004. Personal experience with four kinds of chemical structure drawing software: review on ChemDraw, ChemWindow, ISIS/Draw, and ChemSketch. *Journal of chemical information and computer sciences.* 44:1886-1890.
16. Rahimi-Nasrabadi, M., M. Gholivand, H. Batooli, and A. Vatanara. 2009. Chemical composition of the essential oil from leaves and flowering aerial parts of *Psammogeton canescens* (DC.) vake from Iran. . □□□□□□ □□□□□□ □□□□□□ □□□□ □□□□□□□□ 8:82-86.
17. Ramzan, M., M.I. Karobari, A. Heboyan, R.N. Mohamed, M. Mustafa, S.N. Basheer, V. Desai, S. Batool, N. Ahmed, and B. Zeshan. 2022. Synthesis of silver nanoparticles from extracts of wild ginger (*Zingiber zerumbet*) with antibacterial activity against selective multidrug resistant oral bacteria. *Molecules.* 27:2007.
18. Tariq, F., N. Ahmed, M. Afzal, M.A.U. Khan, and B. Zeshan. 2020. Synthesis, Characterization and antimicrobial activity of *Bacillus subtilis*-derived silver nanoparticles against multidrug-resistant bacteria. *Jundishapur Journal of Microbiology.* 13.
19. Tundis, R., M.R. Loizzo, and F. Menichini. 2010. Natural products as α -amylase and α -glucosidase inhibitors and their hypoglycaemic potential in the treatment of diabetes: an update. *Mini reviews in medicinal chemistry.* 10:315-331.
20. Uddin, G., A. Rauf, M. Arfan, Waliullah, I. Khan, M. Ali, M. Taimur, I. Ur-Rehman, and Samiullah. 2012. Pistagremic acid a new leishmanicidal triterpene isolated from *Pistacia integerrima* Stewart. *Journal of enzyme inhibition and medicinal chemistry.* 27:646-648.
21. Wargasetia, T.L., S. Permana, and N. Widodo. 2018. Potential use of compounds from sea cucumbers as MDM2 and CXCR4 inhibitors to control cancer cell growth. *Experimental and therapeutic Medicine.* 16:2985-2991.